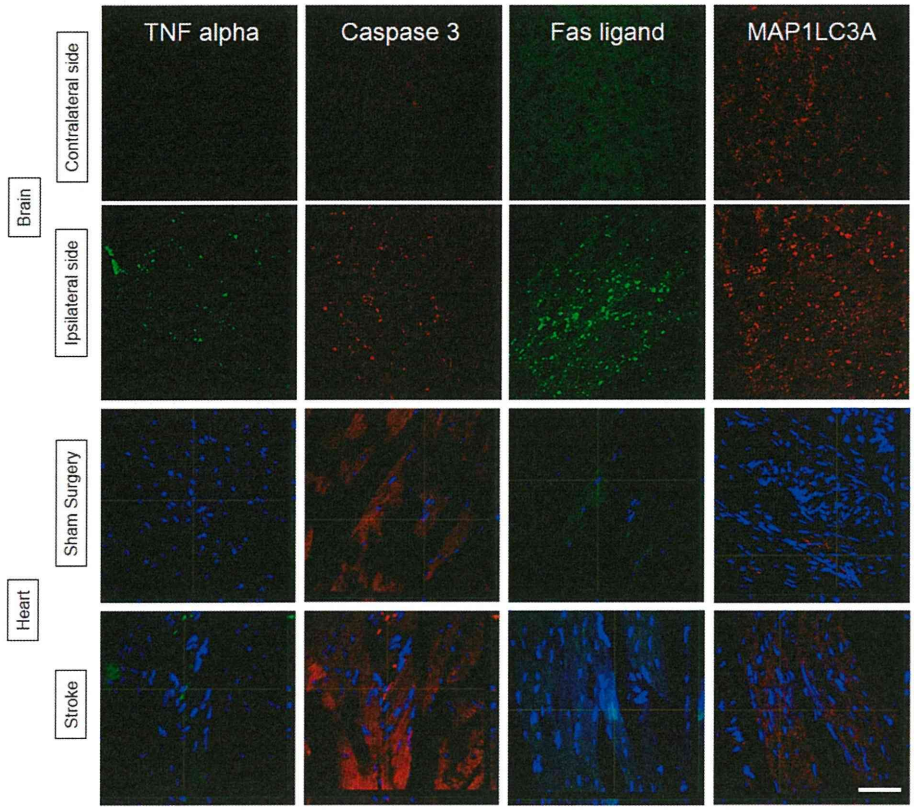


| | | TNF alpha | Caspase 3 | Fas ligand | MAP1LC3A |
|---|---|---|---|---|---|
| Brain | Contralateral side | - | + | - | + |
| | Ipsilateral side | +++ | +++ | +++ | +++ |
| Heart | Sham | - | + | - | + |
| | Stroke | + | ++ | + | +++ |

**Figure 4.** Immunohistochemical analyses of brain and heart in ischemic stroke rats. In the brain, necrotic, apoptotic, and autophagic cells were mostly detected in the ischemic stroke ipsilateral hemisphere. Whereas Caspase 3 and MAP1LC3A were observed in both hemispheres, the contralateral side immunoreactivity was less intense than ipsilateral side. The heart from the ischemic stroke animal also displayed all cell death markers. The immunoreactivity in sham animals was less intense than in stroke animals. Scale bar represents 50 μm. TNF-α indicates tumor necrosis factor-α.

## Acknowledgments

Dr Ishikawa, J. Vasconcellos, and Dr Borlongan conceived the research theme and the experimental design and wrote the first draft of the manuscript. Dr Ishikawa, Dr Tajiri, J. Vasconcellos, and Dr Borlongan performed the experiments. All the authors edited and approved the final manuscript.

## Sources of Funding

Dr Borlongan is supported by the National Institutes of Health, the National Institute of Neurological Disorders and Stroke 1R01NS071956-01, Department of Defense W81XWH-11-1-0634, and the James and Esther King Foundation for Biomedical Research Program 1KG01-33966.

## Disclosures

None.

## References

1. Centers for Disease Control and Prevention (CDC). Prevalence of coronary heart disease--united states, 2006–2010. *MMWR Morb Mortal Wkly Rep*. 2011;60:1377–1381.
2. Centers for Disease Control and Prevention (CDC). Prevalence of stroke--united states, 2006–2010. *MMWR Morb Mortal Wkly Rep*. 2012;61:379–382.
3. Kannel WB. The Framingham Study: ITS 50-year legacy and future promise. *J Atheroscler Thromb*. 2000;6:60–66.
4. Lo EH, Dalkara T, Moskowitz MA. Mechanisms, challenges and opportunities in stroke. *Nat Rev Neurosci*. 2003;4:399–415.
5. Zhang ZG, Chopp M. Neurorestorative therapies for stroke: underlying mechanisms and translation to the clinic. *Lancet Neurol*. 2009;8:491–500.
6. Lawlor DA, Smith GD, Leon DA, Sterne JA, Ebrahim S. Secular trends in mortality by stroke subtype in the 20th century: a retrospective analysis. *Lancet*. 2002;360:1818–1823.
7. Oppenheimer SM, Hachinski VC. The cardiac consequences of stroke. *Neurol Clin*. 1992;10:167–176.
8. Prosser J, MacGregor L, Lees KR, Diener HC, Hacke W, Davis S; VISTA Investigators. Predictors of early cardiac morbidity and mortality after ischemic stroke. *Stroke*. 2007;38:2295–2302.
9. Klingelhöfer J, Sander D. Cardiovascular consequences of clinical stroke. *Baillieres Clin Neurol*. 1997;6:309–335.
10. Adams JE III, Abendschein DR, Jaffe AS. Biochemical markers of myocardial injury. Is MB creatine kinase the choice for the 1990s? *Circulation*. 1993;88:750–763.
11. Snider SR, Kuchel O. Dopamine: an important neurohormone of the sympathoadrenal system. Significance of increased peripheral dopamine release for the human stress response and hypertension. *Endocr Rev*. 1983;4:291–309.
12. Ay H, Koroshetz WJ, Benner T, Vangel MG, Melinosky C, Arsava EM, et al. Neuroanatomic correlates of stroke-related myocardial injury. *Neurology*. 2006;66:1325–1329.
13. Cechetto DF, Wilson JX, Smith KE, Wolski D, Silver MD, Hachinski VC. Autonomic and myocardial changes in middle cerebral artery occlusion: stroke models in the rat. *Brain Res*. 1989;502:296–305.
14. Matsukawa N, Yasuhara T, Hara K, Xu L, Maki M, Yu G, et al. Therapeutic targets and limits of minocycline neuroprotection in experimental ischemic stroke. *BMC Neurosci*. 2009;10:126.

15. Bell E, Cao X, Moibi JA, Greene SR, Young R, Trucco M, et al. Rapamycin has a deleterious effect on MIN-6 cells and rat and human islets. *Diabetes*. 2003;52:2731–2739.
16. Kaneko Y, Tajiri N, Su TP, Wang Y, Borlongan CV. Combination treatment of hypothermia and mesenchymal stromal cells amplifies neuroprotection in primary rat neurons exposed to hypoxic-ischemic-like injury *in vitro*: role of the opioid system. *PLoS One*. 2012;7:e47583.
17. Borlongan CV, Hadman M, Sanberg CD, Sanberg PR. Central nervous system entry of peripherally injected umbilical cord blood cells is not required for neuroprotection in stroke. *Stroke*. 2004;35:2385–2389.
18. Borlongan CV, Skinner SJ, Geaney M, Vasconcellos AV, Elliott RB, Emerich DF. Intracerebral transplantation of porcine choroid plexus provides structural and functional neuroprotection in a rodent model of stroke. *Stroke*. 2004;35:2206–2210.
19. Go AS, Mozaffarian D, Roger VL, Benjamin EJ, Berry JD, Borden WB, et al; American Heart Association Statistics Committee and Stroke Statistics Subcommittee. Heart disease and stroke statistics–2013 update: a report from the American Heart Association. *Circulation*. 2013;127:e6–e245.
20. Micheli S, Agnelli G, Caso V, Alberti A, Palmerini F, Venti M, et al. Acute myocardial infarction and heart failure in acute stroke patients: frequency and influence on clinical outcome. *J Neurol*. 2012; 259:106–110.
21. Tokgözoglu SL, Batur MK, Top uoglu MA, Saribas O, Kes S, Oto A. Effects of stroke localization on cardiac autonomic balance and sudden death. *Stroke*. 1999;30:1307–1311.
22. Korpelainen JT, Sotaniemi KA, Myllylä VV. Autonomic nervous system disorders in stroke. *Clin Auton Res*. 1999;9:325–333.
23. Oppenheimer SM, Kedem G, Martin WM. Left-insular cortex lesions perturb cardiac autonomic tone in humans. *Clin Auton Res*. 1996;6:131–140.
24. Sander D, Klingelhöfer J. Changes of circadian blood pressure patterns after hemodynamic and thromboembolic brain infarction. *Stroke*. 1994;25:1730–1737.
25. Min J, Farooq MU, Greenberg E, Aloka F, Bhatt A, Kassab M, et al. Cardiac dysfunction after left permanent cerebral focal ischemia: the brain and heart connection. *Stroke*. 2009;40:2560–2563.
26. Dutta P, Courties G, Wei Y, Leuschner F, Gorbatov R, Robbins CS, et al. Myocardial infarction accelerates atherosclerosis. *Nature*. 2012;487:325–329.
27. Kostulas N, Kivisäkk P, Huang Y, Matusevicius D, Kostulas V, Link H. Ischemic stroke is associated with a systemic increase of blood mononuclear cells expressing interleukin-8 mRNA. *Stroke*. 1998;29:462–466.
28. Mo X, Li T, Ji G, Lu W, Hu Z. Peripheral polymorphonuclear leukocyte activation as a systemic inflammatory response in ischemic stroke. *Neurol Sci*. April 26, 2013. doi:10.1007/s10072-013-1447-0.: http://link.springer.com/article/10.1007%2Fs10072-013-1447-0. Accessed July 25, 2013.
29. Wira CR III, Rivers E, Silver B, Lewandowski C. The impact of cardiac contractility on cerebral blood flow in ischemia. *West J Emerg Med*. 2011;12:227–232.
30. Paczkowska E, Gołąb-Janowska M, Bajer-Czajkowska A, Machalińska A, Ustianowski P, Rybicka M, et al. Increased circulating endothelial progenitor cells in patients with haemorrhagic and ischaemic stroke: the role of Endothelin-1. *J Neurol Sci*. 2013;325:90–99.
31. Sörös P, Hachinski V. Cardiovascular and neurological causes of sudden death after ischaemic stroke. *Lancet Neurol*. 2012;11:179–188.
32. DeVries AC, Craft TK, Glasper ER, Neigh GN, Alexander JK. 2006 Curt P. Richter award winner: Social influences on stress responses and health. *Psychoneuroendocrinology*. 2007;32:587–603.
33. Ning M, Lo EH, Ning PC, Xu SY, McMullin D, Demirjian Z, et al. The brain's heart—therapeutic opportunities for patent foramen ovale (PFO) and neurovascular disease. *Pharmacol Ther*. 2013;139:111–123.

*The Laryngoscope*


# Functional Regeneration of Laryngeal Muscle Using Bone Marrow–Derived Stromal Cells

Shin-ichi Kanemaru, MD, PhD; Yoshiharu Kitani, MD, PhD; Satoshi Ohno, MD, PhD; Taeko Shigemoto, MS; Tsuyoshi Kojima, MD; Seiji Ishikawa, MD; Masanobu Mizuta, MD; Shigeru Hirano, MD, PhD; Tatsuo Nakamura, MD, PhD; Mari Dezawa, MD, PhD

**Objectives/Hypothesis:** To investigate the functional efficiency of skeletal muscles regenerated by transplantation of bone marrow–derived stromal cells (BSCs) or induced-muscle progenitor cells (IMCs) as assessed in the canine posterior cricoarytenoid (PCA) muscle injury model.

**Study Design:** Prospective animal experiment with control.

**Methods:** We performed BSC/IMC transplantation into injured canine PCA muscles. We investigated the capability of auto- and allo-BSC/IMC transplantation using a gelatin sponge scaffold to promote functional regeneration of PCA muscles. Transplantation was assessed by fiberscopic analysis of vocal fold movement. We also examined the histologic changes of the transplanted regions. As a control, a gelatin sponge scaffold without additional cells was transplanted into the injured area.

**Results:** Auto-BSC/IMC transplantation effectively restored vocal fold movement, whereas scaffold alone or allo-BSC/IMC transplantation did not. Histologic examination revealed that (in cases of good recovery) muscle regeneration occurred in the area of cell transplantation, and scar formation without muscle regeneration was observed under control conditions. The dogs with autologous transplantation of BSC had faster functional recovery than did dogs treated with autologous transplantation of IMC.

**Conclusions:** Functional efficiency was shown in skeletal muscles regenerated using BSCs and IMPs. Motor function recovery was observed using autologous transplantation of BSCs and IMCs. Minimal functional recovery was observed using allogeneic transplantation of these cells.

**Key Words:** Mesenchymal stem cells, muscle regeneration, induced muscle progenitor cells, posterior cricoarytenoid muscle, vocal fold.

**Level of Evidence:** NA.

***Laryngoscope*, 123:2728–2734, 2013**

## INTRODUCTION

When muscle injuries occur due to disease or trauma, they might not always be fatal but can lead to functional impairment. Conventionally, impaired motor function due to muscle injury has mainly been restored by rehabilitation and not tissue repair of the damaged site. However, if muscle tissue regeneration is possible and the original function can be restored, tissue repair is obviously superior to residual tissue assuming the function of the damaged tissue. In addition, tissue repair can potentially be applied clinically to treat incurable muscular degenerative diseases such as muscular dystrophy.

Dezawa et al. reported that mesenchymal stem cells (MSCs) can be induced to differentiate into muscle tissue under appropriate conditions.[1] Bone marrow–derived stromal cells (BSCs) consist primarily of MSCs. In previous animal experiments using a vocal fold injury model, we performed BSC transplantation and achieved regeneration of the vocal fold.[2,3] In our present study, functional efficiency was examined in skeletal muscles regenerated using BSCs.

Vocal folds were selected as the target organ to show the recovery of function of regenerated muscle. We focused on the posterior cricoarytenoid (PCA) muscle, the only glottal abductor among the four intrinsic laryngeal muscles. The PCA muscle originates from the posterior surface of the cricoid lamina, runs superiolaterally, and inserts into the muscular process of the arytenoid cartilage. The PCA muscle is innervated by the recurrent laryngeal nerve, and contraction of this muscle

From the Foundation for Biomedical Research and Innovation (S.-I.K.), Kobe, Japan, Department of Otolaryngology–Head and Neck Surgery, Medical Research Institute, Kitano Hospital (S.-I.K.), Osaka; Department of Otolaryngology–Head and Neck Surgery, Graduate School of Medicine (Y.K., S.O., T.K., S.I., M.M., S.H.), Kyoto University, Kyoto; Department of Stem Cell Biology and Histology, Tohoku University Graduate School of Medicine (T.S., M.D.), Sendai; and Department of Bioartificial Organs, Institute for Frontier Medical Sciences (T.N.), Kyoto University, Kyoto, Japan

Editor's Note: This Manuscript was accepted for publication January 28, 2013.

Presented at the American Laryngological Association Annual Meeting, San Diego, California, U.S.A., April 18–22, 2012.

This study was supported by a Health Sciences Research Grant from the Ministry of Health, Labor and Welfare of Japan and the National Institute of Biomedical Innovation in Japan, 2010 research project title "Development of Basic Treatment for Neurological and Muscular Degenerative Diseases Using Autologous Cells and Cells From Cell Banks." The authors have no other funding, financial relationships, or conflicts of interest to disclose.

Send correspondence to Shin-ichi Kanemaru MD, PhD, Department of Otolaryngology, Head and Neck Surgery, Medical Research Institute, Kitano Hospital, 2-4-20 Ohgimachi, Kitaku, Osaka, 530-8480, Japan. E-mail: kanemaru@ent.kuhp.kyoto-u.ac.jp

**DOI: 10.1002/lary.24060**

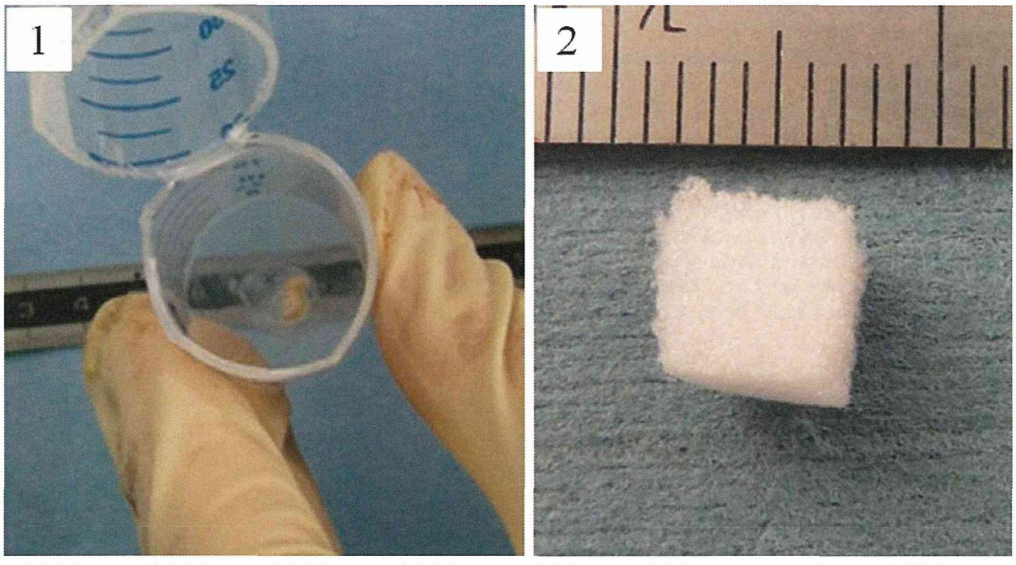


Fig. 1. (A) Transplanted bone marrow–derived stromal cells. (B) Gelatin sponge.

pulls the muscular process of the arytenoid cartilage. This action causes the arytenoid cartilage to rotate, displacing the vocal process laterally and resulting in the abduction of the glottis. Thus, resection of the PCA muscle belly prevents the abduction of the glottis without other effects. In addition, the PCA muscle is suitable for muscle regeneration because its anatomic positional relationship makes it difficult for the scaffold to shift. Because the PCA muscle is very small, the number of cells required for regeneration is relatively small. Regeneration can be directly examined by observation of vocal fold movements using a laryngeal fiberscope. Based on this rationale, we used the PCA muscle injury model. BSCs or induced-muscle progenitor cells (IMCs) were transplanted, and examination was performed to determine whether the regenerated PCA muscles functioned effectively to abduct the vocal fold.

This is the first report of functional regeneration of skeletal muscle in a large animal.

## MATERIALS AND METHODS

This study was performed in accordance with the animal experiment manual of the Animal Research Committee of the Kyoto University.

### *Cells*

One milliliter of bone marrow was harvested from the forelimb humerus of each adult beagle dog (body weight, 8–12 kg). Fetal bovine serum 10% (FBS; Invitrogen, Carlsbad, CA) was added to Dulbecco's modified Eagle's medium (D-MEM; Gibco, Life Technologies, Inc., Grand Island, NY) to yield 15 mL of culture medium. This medium was placed in a 200-mL culture flask and placed in an incubator (MCO-17AIC; Sanyo Co., Osaka, Japan) at 37°C in 5% $CO_2$ atmosphere for 48 hours. The culture medium was replaced with fresh medium while leaving the cells attached to the bottom surface of the flask. The medium was replaced every 3 days, and the level of cell proliferation was examined under an optical microscope (Olympus, IX70; Olympus Co., Tokyo, Japan). On day 14, the cells were confirmed to have completely covered the bottom of the flask. Two milliliters of trypsin/0.25% EDTA (EDTA; Invitrogen) was added to the culture medium, and the cells attached to the bottom surface of the flask were removed. Five minutes later, the trypsin was neutralized with 10 mL of D-MEM + 10% FBS. Subsequently, a cell counter was used to confirm that there were approximately $4 \times 10^6$ cells, and these cells were collected. The resulting cells were centrifuged at 3,500 rpm for 3 minutes (Fig. 1A). For direct transplantation, $5 \times 10^5$ of these cells were adsorbed to a scaffold of gelatin sponge and then transplanted.

When IMCs were used, centrifuged cells were collected, and the method of Dezawa et al.[1] was subsequently used to induce differentiation of BSCs. In the same way as in direct transplantation, transplantation was performed in the resected site of the PCA muscle belly. Both BSCs and IMCs were divided into two groups: a group with autologous (auto) transplantation and another group with allogeneic (allo) transplantation. Allogeneic transplantation was performed by similar methods but with use of cells from another beagle instead of autologous cells. No immunosuppressant was used. In the controls, a gelatin sponge scaffold was soaked with physiologic saline and transplanted.

### *Scaffold*

The gelatin sponge (Spogel; Astellas Co., Tokyo, Japan) used as a scaffold is made by aqueous extraction with heating of crude collagen. This crude collagen is acid- or alkali-treated collagen from animal bones, skin, ligaments, or tendons. The resulting product is lyophilized and sterilized to yield a porous gelatin sponge. The triple helix structure of a collagen molecule unfolds due to thermal denaturation. The main ingredient of the gelatin sponge is a mixture of the denatured products (Fig. 1B).

### *Surgical Procedure and Cell Transplantation*

Each beagle was placed under general anesthesia using intramuscular ketamine hydrochloride (50 mg/kg) (Ketaral; Sankyo Co., Tokyo, Japan) and xylazine (2.0 mg/kg) (Ceractal; Bayer, Tokyo, Japan). An incision of approximately 10 cm was made in the anterior neck to reach the larynx. The thyroid

cartilage was retracted and the PCA muscle was exposed. The entire PCA muscle of the left or the right side was placed in clear view, and the muscle was resected near the midportion of the muscle belly (Fig. 2A). Subsequently, the previously exposed ipsilateral recurrent laryngeal nerve was electrically stimulated. Compound muscle action potentials were measured with electrodes inserted into the distal area of the resected PCA muscle. A gelatin sponge was placed at the resection site. This sponge had been soaked with physiologic saline or the aforementioned cells (autologous BSCs, allogeneic BSCs, autologous IMCs, or allogeneic IMCs). Drops of fibrin glue (Bolheal; Kaketsuken, Kumamoto, Japan) were used for fixation (Fig. 2B). The thyroid cartilage was returned to its original position, and the skin was sutured.

### *Evaluations*

Evaluations involved compound muscle action potential (CMAP) measurements (using MEM-7202 Neuropac 2; Nihon Kohden Corporation, Tokyo, Japan) for electrophysiologic evaluation, vocal fold movements using a video endoscope, and histologic specimens.

In the transplantation procedure (described earlier), CMAPs were measured just before and immediately after resection of the PCA muscle (Fig. 2 and 3). The loss of muscle function was confirmed (Fig. 3). Six months after the treatment, we measured CMAPs in all cases and determined whether or not PCA muscle motor function had been recovered.

An electronic video-endoscope system (BF type1T 240, CV240, CLV-U40D, Olympus Co., Tokyo, Japan) was used to observe vocal fold movements, and the loss of movement was confirmed after resection of the PCA muscle on the surgical side. Subsequently, vocal fold movements were checked over time with a video endoscope as an indicator of restoration of function. Moreover, to quantitate the recovery of vocal fold movement, we measured the ratio of the opening angle of the bilateral vocal folds using a video endoscope under sedation 6 months after the treatment (Fig. 4). We used this ratio to define complete recovery (more than 90%), partial recovery (20% to 90%), and no recovery (less than 20%).

Histopathologic specimens of the PCA muscles were prepared. Comparisons were made between the specimens of the cell transplantation and those of the controls.

## RESULTS

### *Functional Recovery*

Images from the video endoscope in Figure 4 show recovery of the left vocal fold's movement 6 months after autotransplantation of BSCs. Figure 4A and 4B show the left vocal fold immobile, but 6 months later, movement of the left vocal fold had recovered (Fig. 4C and 4D).

Figure 5 shows CMAPs 6 months after the treatment. In this figure, we could confirm the recovery of the PCA muscle motor function by electrophysiologic evaluation.

Table I shows the presence or absence of motor function recovery of the vocal folds using a video endoscope (n = 13) and the recovery rate of vocal fold movement. Motor function recovery was achieved using autotransplantation of BSCs and IMCs, but minimal or no motor function recovery was achieved using allotransplantation of either type of cell. Motor function recovery was not observed in any dog in the control group. The CMAP data were in accordance with the results of Table I.

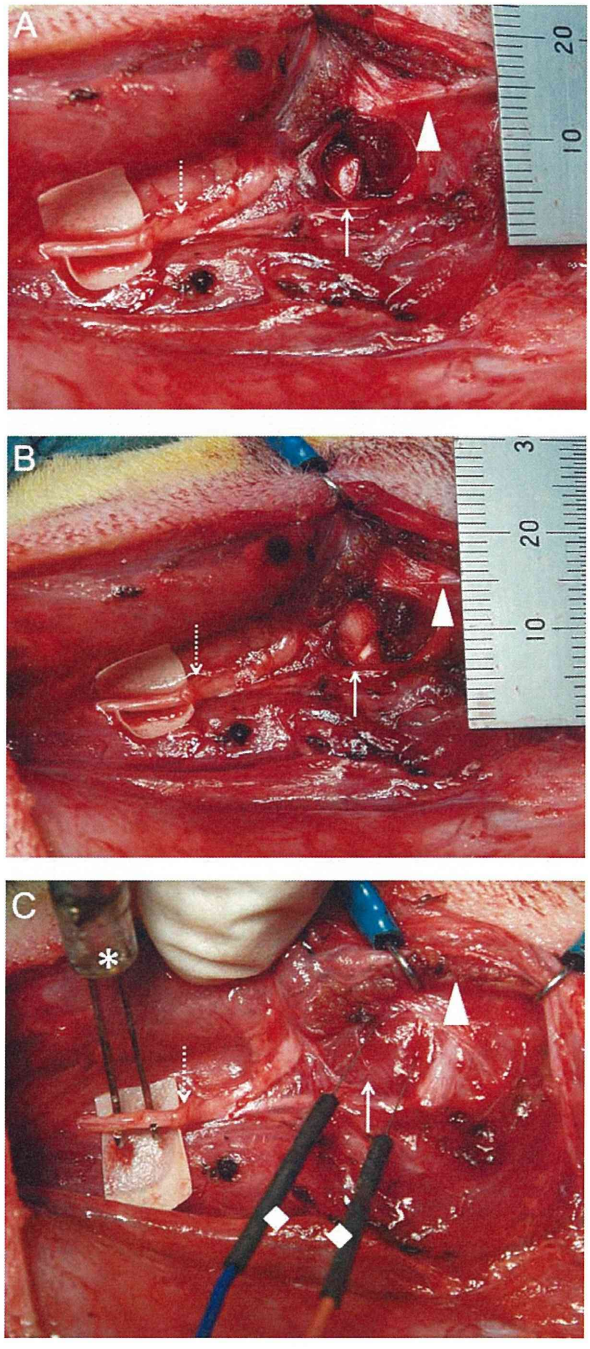


Fig. 2. (A) Exposure and resection of the posterior cricoarytenoid (PCA) muscle. Arrow: resected site of the PCA muscle; dashed arrow: recurrent laryngeal nerve; triangle: thyroid cartilage. (B) Transplantation of cells and scaffold. Arrow: transplanted cells and scaffold at the resected site of the PCA muscle; dashed arrow: recurrent laryngeal nerve; triangle: thyroid cartilage. (C) Measurement of compound muscle action potentials before resection of the PCA muscle. Arrow: resected site of the PCA muscle; dashed arrow: recurrent laryngeal nerve; triangle: thyroid cartilage; asterisk: nerve stimulator; diamond; needle electrode.

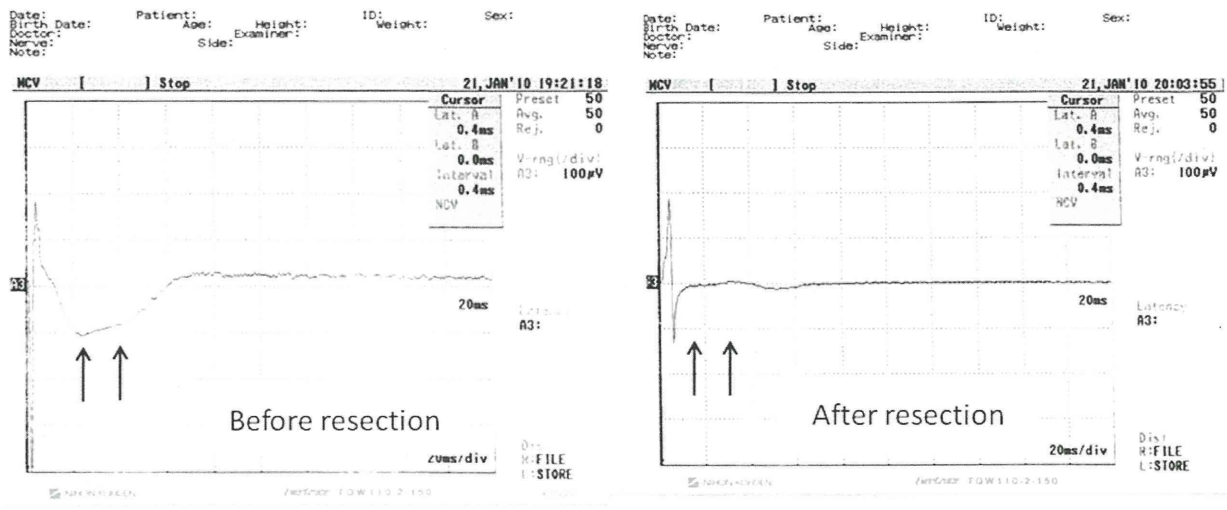


Fig. 3. Compound muscle action potentials (CMAPs) before and after resection; CMAP (arrow) was observed before resection but disappeared after resection.

The time required for functional recovery was compared for dogs with auto-BSC transplantation versus dogs with auto-IMC transplantation. The time required was approximately 2 months versus 3 to 4 months, respectively.

### *Histology*

Figures 6 and 7 show the histopathologic specimens. In dogs with functional recovery, there was connective tissue in some areas of the transplanted site, and muscle regeneration was observed. In the control group, we observed the proliferation of irregular connective tissue to a much greater extent than observed with dogs undergoing functional recovery at the site of transplantation.

## DISCUSSION

There have been many reports about the ability of MSCs to differentiate into muscles or mesodermal

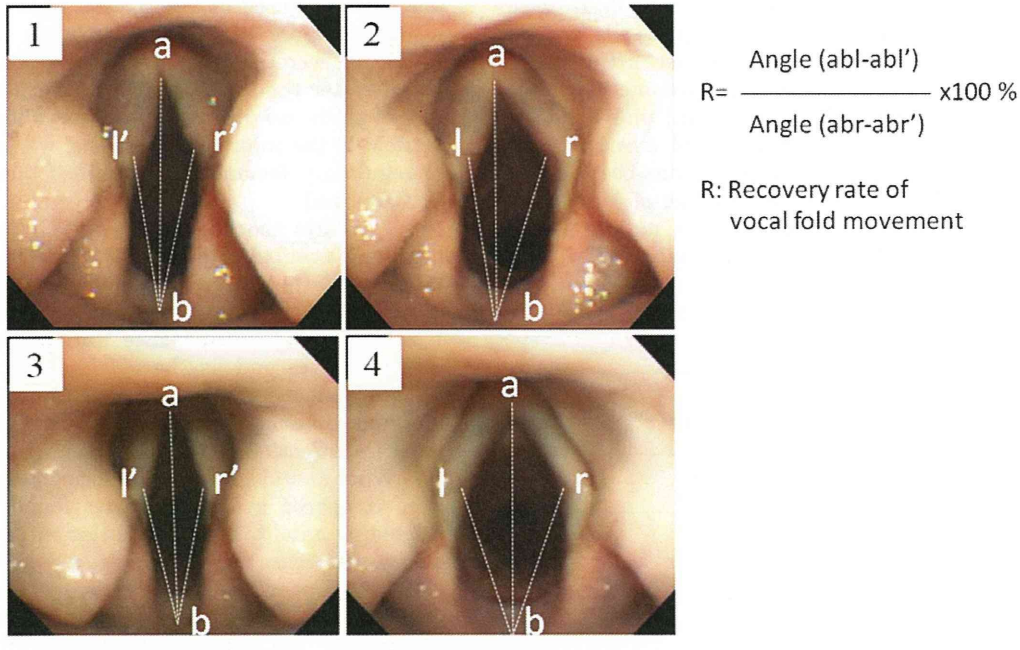


Fig. 4. Images from the video endoscope. (A, B) Immediately after resection of posterior cricoarytenoid muscle. (C, D) Six months after autotransplantation of bone marrow–derived stromal cells to the left side. We defined the recovery rate of vocal fold movement. A = anterior commissure; b = midportion of interarytenoid area; r, l (r', l') = junctional region of arytenoid cartilage and vocal ligament at opening position (r, l) and at resting respiratory position.

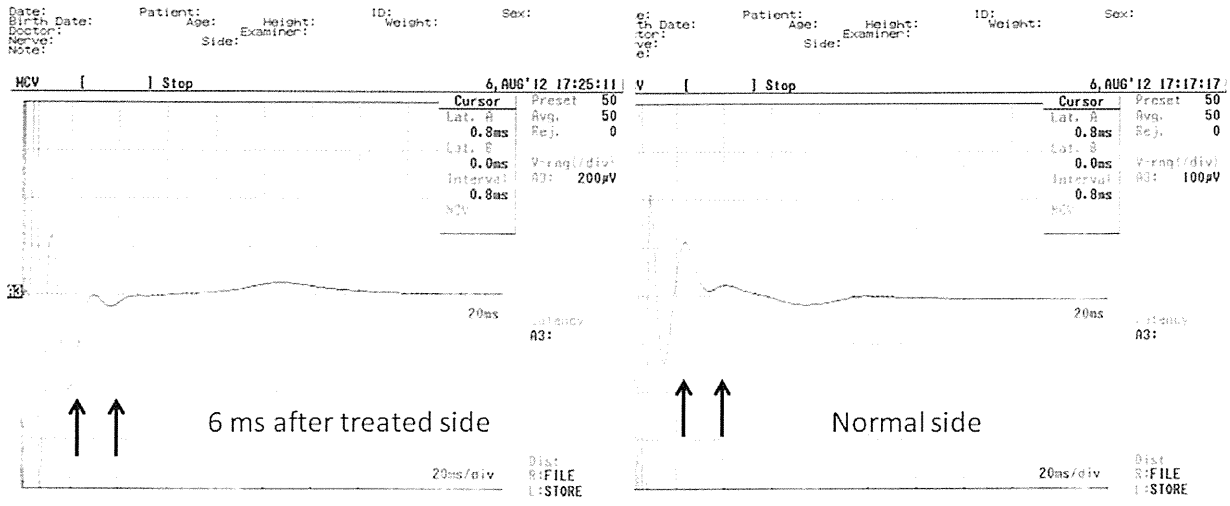


Fig. 5. Compound muscle action potentials (CMAPs) 6 months after autologous bone marrow–derived stromal cells, treated side and normal side in the same canine. CMAP (arrow) of the treated side recovered to the same extent as that of the normal side.

tissue.[4,5] However, Dezawa et al. were the first to develop a method for future clinical application which enabled MSCs to reliably differentiate into muscles.[1]

Some reports have shown that regenerated muscles regained their original functions, but these reports involved cardiac muscle functions of large animals or skeletal muscle motor functions of mice and rats.[6] Skeletal motor functions in mice and rats are more easily observed as recovery of lower limb movement. Restoration of skeletal motor function has not been shown in large animals. Large animals have not been used because for functional restoration of muscle cells, several things need to happen: 1) a large number of transplant cells need to be prepared, 2) regenerated muscle tissue needs to move consistently as one unit, and 3) motor function recovery needs to be observed clearly. These issues pose very difficult challenges. It has been known that telomeres shorten after each division of MSCs, and there are limitations to their division and proliferation.[7,8] Thus, it is very difficult to obtain cells in the range of 100 million. When BSCs are subcultured, the cell count does not increase beyond a certain number of generations. Many problems arise in efforts to demonstrate functional restoration of regenerated muscle. However, we found that the PCA muscle is an ideal target organ that meets all of the above conditions. Therefore, we selected vocal folds as a target organ to show functional recovery of regenerated muscle as described in the introduction.

When tissue regeneration is performed, an appropriate environment is normally necessary for the three components of regeneration: cells, scaffold, and regulatory factors. Based on the concept of in situ tissue engineering, we predicted that some type of growth factor would be secreted from the surroundings of the PCA muscle after the trigger of PCA muscle resection. Thus, in this study, we directly transplanted only the cells and scaffold to the injured PCA muscle without the addition of regulatory factors and examined whether regeneration occurred.

A gelatin sponge has a relatively sparse structure, providing scaffold and spaces for cells to freely grow. When a gelatin sponge is imbedded in the tissue or body cavity, it liquefies and is absorbed within approximately 1 month.[9] A gelatin sponge adheres strongly to the wound surface and has been found to have similar hemostatic effects as fibrin.[10] A gelatin sponge has been reported to be useful as a scaffold in regenerative treatment in patients with tympanic membrane perforation.[11]

When autologous and allogeneic cell transplants were compared in our study, we found that the group treated by autologous transplantation had functional recovery, whereas the group receiving allogeneic transplants had poor functional recovery. This result could have occurred because the transplanted cells were rejected by the recipients. However, there are many reports that MSCs possess immunomodulatory properties.[12,13] MSCs are immunosuppressive, interacting with T lymphocytes, antigen-presenting cells, B lymphocytes,

TABLE I.
Functional Recovery of the Posterior Cricoarytenoid Muscle (N = 13).

| | Complete Recovery | Partial Recovery | No Recovery |
|---|---|---|---|
| Auto-BSCs | 3 | | |
| Allo-BSCs | | | 2 |
| Auto-IMCs | 1 | 2 | |
| Allo-IMCs | | 1 | 1 |
| Control | | | 3 |

Allo = allogeneic; Auto = autologous; BSC = bone marrow–derived stromal cell; IMC = induced-muscle progenitor cell.

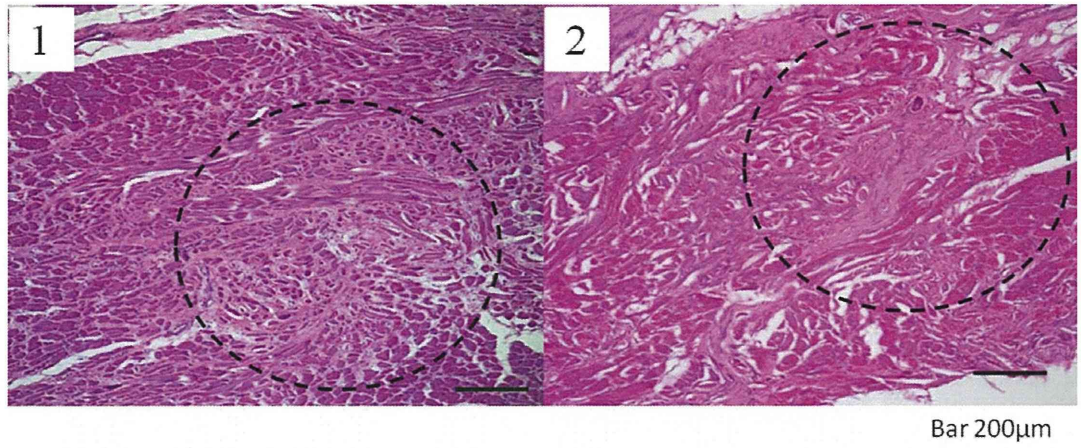


Fig. 6. Pathologic specimens 6 months after resection of posterior cricoarytenoid muscle and transplantation (hematoxylin and eosin stain). The black dotted line is the resected site of the muscle. (A) Dog with autologous bone marrow–derived stromal cell transplantation and functional recovery. (B) Control without functional recovery.

and natural killer cells. In addition, they are immunoprivileged, allowing transplantation across allogeneic barriers.[13] Our result contradicts the anticipated properties of MSCs. It is possible that other cells present in the MSC preparations may have caused rejection by the recipients. If muscle regeneration is to be applied to muscular degenerative diseases such as muscular dystrophy, allogeneic transplants will be necessary. Therefore, use of immunosuppressants might be required in the allogeneic transplantation group, an approach we will investigate in the next round of studies. Furthermore, there has been a report that MSCs promote malignant tumor formation.[14] Thus, this treatment methodology should not be applied for regeneration of muscle after resection of malignant tumors. However, clinical application of this method may still include a wide range of diseases and injuries.

Functional recovery was observed approximately 2 months after transplantation in the auto-BSC group and approximately 3 to 4 months after transplantation in the auto-IMC group, indicating faster recovery in the auto-BSC group. This finding suggested that the effects of transplanted cells in the process of muscle regeneration differed between these two groups. Based on our previous study,[3] we speculated that in auto-BSC transplantation, the transplanted cells remained as is without differentiation and that the following occurred simultaneously: the transplanted cells contributed to the improvement of the regenerative environment by paracrine and autocrine actions, and the transplanted cells directly differentiated into muscle tissue at the transplanted site. In the auto-IMC transplantation, it was thought that direct differentiation into muscle tissue occurred at the transplanted site without paracrine or autocrine action. More time

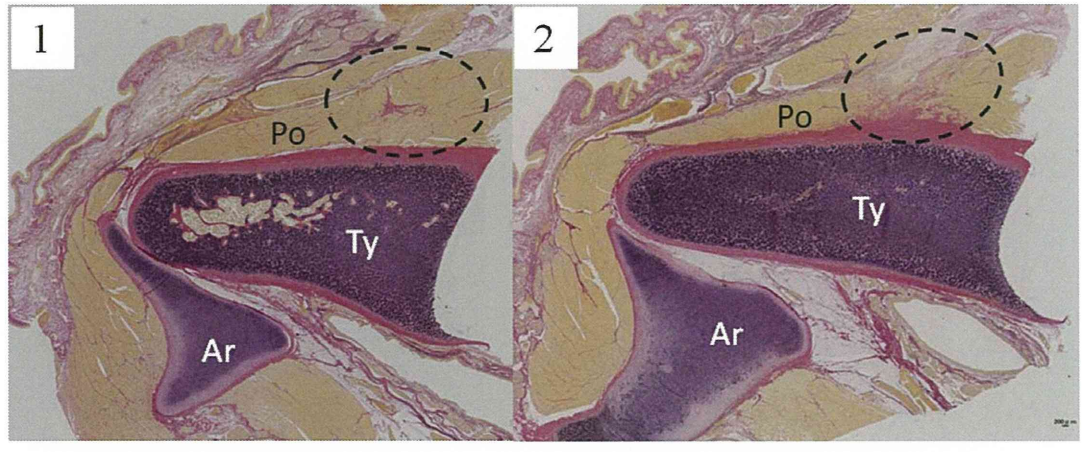


Fig. 7. Pathologic specimens 6 months after resection of the posterior cricoarytenoid muscle and transplantation (Elastica van Gieson stain). (A) Dog with autologous bone marrow–derived stromal cell transplantation and functional recovery. (B) Control without functional recovery. Dotted line indicates collagen fibers such as collagen stained pink. The dogs with good functional recovery had narrower scarred areas compared to those with poor functional recovery. Ar = arytenoid cartilage; Po = posterior cricoarytenoid muscle; Ty = thyroid cartilage.

might be required to achieve sufficient muscle regeneration and functional restoration using transplanted cells only. BSCs have a great potential for contributing paracrine and autocrine factors. However, this potential may be lost in proportion to BSCs' differentiation. Therefore, it is possible that IMCs have already lost this capacity.

Future topics of study include examination of the roles of transplanted cells.

## CONCLUSION

Functional efficiency was shown in skeletal muscles regenerated using BSCs and induced muscle progenitor cells. Motor function recovery was observed using autologous transplantation of BSCs and induced muscle progenitor cells. Minimal functional recovery was observed using allogeneic transplantation of these cells. Muscle tissue regeneration in the transplanted site was observed in dogs with functional recovery after BSC transplantation. In the control group, instead of muscle regeneration, proliferation of irregular connective tissue was observed at the site of transplantation. The dogs with autologous transplantation of BSCs had faster functional recovery compared to dogs with autologous transplantation of induced muscle progenitor cells.

## BIBLIOGRAPHY


1. Dezawa M, Ishikawa H, Itokazu Y, et al. Bone marrow stromal cells generate muscle cells and repair muscle degeneration. *Science* 2005;309:314–317.
2. Kanemaru S, Nakamura T, Kojima H, et al. Regeneration of the vocal cord using autologous mesenchymal stem cells. *Ann Otol Rhinol Laryngol* 2003;112:915–920.
3. Kanemaru S, Nakamura T, Yamashita M, et al. Destiny of the autologous bone marrow derived stromal cells implanted in the vocal fold. *Ann Otol Rhinol Laryngol* 2005;114:907–912.
4. Grove JE, Bruscia E, Krause DS. Plasticity of bone marrow-derived stem cells. *Stem Cell* 2004;22:487–500.
5. Beyer Nardi N, da Silva Meirelles L. Mesenchymal stem cells: isolation, in vitro expansion and characterization. *Handb Exp Pharmacol* 2006;249–282. http://www.ncbi.nlm.nih.gov/pubmed/16370331.
6. Winkler T, von Roth P, Matziolis G, et al. Dose-response relationship of mesenchymal stem cell transplantation and functional regeneration after severe skeletal muscle injury in rats. *Tissue Eng Part A* 2009;15:487–492.
7. Baxter MA, Wynn RF, Jowitt SN, et al. Study of telomere length reveals rapid aging of human marrow stromal cells following in vitro expansion. *Stem Cells* 2004;22:675–682.
8. Bonab MM, Alimoghaddam K, Talebian F, et al. Aging of mesenchymal stem cell in vitro. *BMC Cell Biol* 2006;10:7–14.
9. Correll JT, Prentice HR, Wise EC. Biological investigations of a new absorbable sponge. *Surg Gynecol Obstet* 1945;81:585–589.
10. Jenkins HP, Janda R, Clarke J. Clinical and experimental observations on the use of gelatin sponge or foam. *Surgery* 1946;20:124–132.
11. Kanemaru S, Umeda H, Kitani Y, et al. Regenerative treatment for tympanic membrane perforation. *Otol Neurotol* 2011;32:1218–1223.
12. Sordi V, Piemonti L. Therapeutic plasticity of stem cells and allograft tolerance. *Cytotherapy* 2011;13:647–660.
13. Larsen S, Lewis ID. Potential therapeutic applications of mesenchymal stromal cells. *Pathology* 2011;43:592–604.
14. Spaeth EL, Dembinski JL, Sasser AK, et al. Mesenchymal stem cell transition to tumor-associated fibroblasts contributes to fibrovascular network expansion and tumor progression. *PLoS One* 2009;4:e4992.

Research article

# Treatment with basic fibroblast growth factor-incorporated gelatin hydrogel does not exacerbate mechanical allodynia after spinal cord contusion injury in rats

**Takeo Furuya[1], Masayuki Hashimoto[1], Masao Koda[1], Atsushi Murata[1], Akihiko Okawa[1], Mari Dezawa[2], Dai Matsuse[2], Yasuhiko Tabata[3], Kazuhisa Takahashi[1], Masashi Yamazaki[1]**

[1]Department of Orthopaedic Surgery, Chiba University Graduate School of Medicine, Chiba, Japan, [2]Department of Anatomy and Neurobiology, Tohoku University Graduate School of Medicine, Sendai, Japan, [3]Department of Biomaterials, Institute for Frontier Medical Sciences, Kyoto University, Kyoto, Japan

Besides stimulating angiogenesis or cell survival, basic fibroblast growth factor (bFGF) has the potential for protecting neurons in the injured spinal cord.

**Objective:** To investigate the effects of a sustained-release system of bFGF from gelatin hydrogel (GH) in a rat spinal cord contusion model.

**Methods:** Adult female Sprague–Dawley rats were subjected to a spinal cord contusion injury at the T10 vertebral level using an IH impactor (200 kdyn). One week after contusion, GH containing bFGF (20 μg) was injected into the lesion epicenter (bFGF – GH group). The GH-only group was designated as the control. Locomotor recovery was assessed over 9 weeks by Basso, Beattie, Bresnahan rating scale, along with inclined plane and Rota-rod testing. Sensory abnormalities in the hind paws of all the rats were evaluated at 5, 7, and 9 weeks.

**Results:** There were no significant differences in any of the motor assessments at any time point between the bFGF – GH group and the control GH group. The control GH group showed significantly more mechanical allodynia than did the group prior to injury. In contrast, the bFGF – GH group showed no statistically significant changes of mechanical withdrawal thresholds compared with pre-injury.

**Conclusion:** Our findings suggest that bFGF-incorporated GH could have therapeutic potential for alleviating mechanical allodynia following spinal cord injury.

**Keywords:** Allodynia, Basic fibroblast growth factor, Scaffold, Spinal cord injuries, Motor deficits, Neuroprotection, Locomotor recovery, Paraplegia

## Introduction

Spinal cord injury (SCI) is the most devastating type of trauma for patients due to the long-lasting disability and limited responses to acute drug administration and efforts at rehabilitation. Previously, we reported on combinational therapy, bone marrow stromal cell (BMSC) transplantation, and Rho-kinase inhibitor administration for spinal cord contusion.[1] Combination therapy showed better recovery than controls, but we detected no synergy between the components of the combination. We counted lower numbers of remaining BMSCs and saw a gradual decrease in the number of BMSCs over the observation period. We hypothesized that we might have observed more locomotor recovery had the remaining cells been more abundant.

Gelatin hydrogel (GH) incorporating basic fibroblast growth factor (bFGF) is one of the more promising tools for treating SCI. bFGF-incorporated GH has enhanced angiogenesis in several experimental models,[2–4] and it has already found some clinical

Correspondence to: Masayuki Hashimoto, Department of Orthopaedic Surgery, Chiba University Graduate School of Medicine, 1-8-1 Inohana, Chuo-ku, Chiba 260-8670, Japan. Email: futre@tg7.so-net.ne.jp


DOI 10.1179/2045772312Y.0000000030

usage, including a phase I/IIa study in humans in the hope of enhancing angiogenesis.[5] Multiple studies have also identified various functions for bFGF itself in damaged central nerve system tissue, including the following: attenuating neurotoxicity and increasing antioxidant enzyme activities in hippocampal neurons;[6] protecting against excitotoxicity and chemical hypoxia in both neonatal and adult rat neurons;[7] preventing the death of lesioned cholinergic neurons *in vivo*;[8] and protecting spinal motor neurons after experimental SCI.[9] These research findings together suggest that bFGF-incorporated GH has the potential for saving damaged neuronal cells and improving angiogenesis after SCI.

BMSC with fibrin scaffolding has been observed to improve survival of transplanted cells after spinal cord hemisection.[10] The combination of the neurotrophin-3, platelet-derived growth factor, and fibrin scaffold has been reported to enhance the total number of neural progenitor cells present in the spinal cord lesion 2 weeks after injury.[11] The study findings together suggest that the controlled release of growth factor incorporated into a scaffold in conjunction with cell transplantation has the potential to improve the survival of transplanted cells and enhancing locomotor recovery after SCI.

In the present study, we sought to establish the safety of bFGF-incorporated GH in humans. Our study protocol was to inject bFGF-incorporated GH and GH without bFGF into contused spinal cords in rats and to measure locomotion for 9 weeks after SCI, as well to estimate two types of allodynia before and after SCI.

## Methods

### *Experimental groups*

The 18 animal subjects were randomly assigned to two groups: (1) the bFGF + GH group (bFGF – GH, $n = 8$), which received an injection of bFGF + GH mixture into the spinal cord; (2) the GH-only group (GH, $n = 10$), which received an injection of GH without bFGF into the spinal cord.

### *bFGF-incorporated GH treatment*

#### bFGF-incorporated GH

A frozen aliquot of bFGF (10 μg/μl) was diluted 1:1 with phosphate-buffered saline (PBS) and incubated overnight at 4°C (5 μg/μl). GH (2 mg) was mixed with a 20-μl aliquot of bFGF and incubated at 37°C for 1 hour. Just before injection, bFGF-incorporated GH was diluted by 20 μl of PBS. We injected 8 μl bFGF-incorporated GH into the injured spinal cord.

#### Animal surgery

Our experimental SCI protocol utilized a total of 18 8-week-old female Sprague–Dawley rats (SLC, Hamamatsu, Japan). Rats were anesthetized with 1.6% halothane in 0.5 l/minute oxygen. We performed a laminectomy at the T9–T10 levels and induced a contusion injury of the spinal cord with the infinite horizon impactor (IH impactor, 200 kdyn, Precision Systems and Instrumentation, Lexington, NY, USA). Rats were group-housed in the animal facility and maintained under conditions of constant temperature and humidity. Food and water were provided *ad libitum*. Manual bladder expression was performed twice a day until recovery of the bladder reflex. All animals were given antibiotics (500 μl/day; Bactramin, Chugai Pharmaceutical, Tokyo, Japan) by subcutaneous administration once a day for 3 days. Body weight after SCI was measured weekly, from which we calculated body weight ratios by dividing each post-injury body weight by the body weight before surgery.

Seven days after injury, we re-exposed the injury site and injected the same volume (8 μl) of bFGF-incorporated GH, or GH only, into the center of the injured spinal cord using a micro-glass pipette needle attached to a 10-μl Hamilton syringe (Hamilton Company, Reno, NV, USA) under microscopy. We performed the injection at multiple depths (2, 1.5, 1.0, and 0.5 mm) during drawback, and the needle was left in the spinal cord for 3 minutes following the last injection in order to minimize reflux. None of the animals showed abnormal behavior. All the experimental procedures were performed in compliance with the guidelines established by the Animal Care and Use Committee of Chiba University.

### *Assessments of sensory motor functions*

#### Basso, Beattie, Bresnahan open field locomotor test

Hind limb function was assessed in an open field (100 cm × 60 cm plastic pool) using the Basso, Beattie, Bresnahan (BBB) open field locomotor test.[12] Measurements were performed weekly thereafter for 9 weeks. Tests were videotaped for 5 minutes and scored by a trained observer who was unaware of the treatment group to which each subject was assigned.

#### Inclined plane test

Each animal was placed in head-up, transverse, and head-down positions on an inclined plane and the angle of slope gradually increased. The angle at which the animal fell down from the slope was recorded for each position, two trials per animal, after SCI. The better of the two trial results for each subject were

combined and compared among the three groups. We performed these measurements before surgery and then 4, 6, and 8 weeks after SCI.

### Rota-rod test

Four and 6 weeks after SCI, animals were placed on a 5 cm-wide turning cylinder (Rota-rod MK-630B, Muromachi Kikai, Japan) and forced to walk on it. The speed of rotation was gradually accelerated from 3 rpm (rotations per minute) to 30 rpm, and then maintained at 30 rpm for 5 minutes (Mode A1, 3–30 rpm). The time when the animal fell from the Rota-rod was recorded. Preoperatively, animals were able to stay on the Rota-rod for a mean duration of 199.3 seconds.

### Sensory tests

Thermal nociceptive thresholds in rat hind limbs were evaluated using a Hargreaves device (Ugo Basile, Varese, Italy). The rats were placed in individual transparent acrylic boxes with the floor maintained at 28°C. A heat stimulus (150 mcal/seconds/$cm^2$) was delivered using a 0.5 cm-diameter radiant heat source positioned under the plantar surface of the hind limb. The heat source was placed alternately under each hind limb to avoid anticipation by the animal. A cutoff time of 22 seconds was used, as we had previously ascertained that no tissue damage would result within this time period. The withdrawal threshold was calculated as the average value of three consecutive tests. Mechanical withdrawal thresholds in rat hind limbs were tested using a dynamic plantar aesthesiometer (Ugo Basile), in which a mechanical stimulus was applied via an actuator filament (0.5 mm diameter), which under computer control applied a linear ramp 5.0 g/seconds to the plantar surface of the hind limb. The withdrawal threshold was calculated as the average of six consecutive tests. Both tests were performed pre-injury and then 5, 7, and 9 weeks after contusion.

### Anterograde labeling of the cortico-spinal tract with biotinylated dextran amine; immunohistochemical; and histological assessments

Nine weeks after contusion, the cortico-spinal tract was bilaterally traced under halothane anesthesia with 2.0 µl biotinylated dextran amine (BDA, molecular weight: 10 000, 10% in 0.01 M PBS, Molecular Probes, Carlsbad, CA). A micro-glass pipette needle attached to a 2-µl Hamilton syringe was stereotaxically guided, and BDA was slowly injected into four sites in the sensorimotor cortex for the hind limb at a 1-mm depth: Bregma 2 mm, sagittal suture 2 mm; Bregma 2 mm, sagittal suture 3 mm; Bregma 2.5 mm, sagittal suture 3 mm; Bregma 2.5 mm, sagittal suture 2.5 mm. The needle was left in place for 1 minute following each injection to minimize reflux.

#### *Histology*

Animals were subjected to trans-cardiac perfusion with 4% paraformaldehyde in PBS (pH 7.4) 14 days after BDA injection. The spinal cords were dissected and immersed overnight in 4% paraformaldehyde and then stored in 20% sucrose in PBS. The spinal cords were cut into 20-mm lengths (10 mm rostral to and 10 mm caudal to the lesion site) and embedded in optimal cutting temperature (OCT) compound (Tissue Tek, Sakura Finetechnical, Tokyo, Japan). We sectioned each block in the sagittal plane (25 µm) using a cryostat and mounted eight consecutive sections on poly-L-lysine-coated slides (Matsunami, Tokyo, Japan) to make serial sections. The sections on each slide were sliced at 150 µm intervals; each eight section slide therefore covered approximately 1200 µm of the lesion site. We performed histological or immunohistochemical staining on the slides.

To evaluate lesion size, we stained three slices from each animal with cresyl violet. We determined the cavity size of each section using Photoshop 5.5 software (Adobe, San Jose, CA, USA). We calculated a mean cavity size from these three values for each animal and compared cavity sizes between groups.

For anterograde labeling of the cortico-spinal tract with BDA, sections were incubated with Alexa Fluor 594-conjugated streptavidin (1:800; Molecular Probes). We selected seven consecutive sections from the rostral edge of the lesion center, which we photographed with a 20× objective lens using a fluorescence microscope (DP71, Olympus, Tokyo, Japan). We added up the number of fibers and compared the fiber counts between the groups.

Three slices per animal, centered on the lesion epicenter, were incubated with rabbit anti-calcitonin gene-related peptide (CGRP) antibody (1:1000, ImmunoStar, Inc. Hudson, WI, USA) or rabbit anti-von Willebrand factor (1:400, Dako Cytomation, Glostrup, Denmark), then reacted with Alexa-Fluor 594 goat anti-rabbit IgG secondary antibody. Slices were photographed on the rostral and caudal edges of the lesion epicenter with a 10× objective lens using a fluorescence microscope (DP71, Olympus). The numbers of CGRP-positive immunoreactive fibers or von Willebrand factor-positive immunoreactive vessels were counted and averaged.

#### *Statistical analysis*

For histological studies and for assessments of sensory motor functions at each time point, we performed a

Mann–Whitney *U* test. For the 9-week locomotor scale, we performed repeated-measures analysis of variance (ANOVA). Data were reported as mean values ± SEM. Differences with *P* values <0.05 were considered statistically significant.

## Results

We measured body weight ratios every week after SCI. Rats were treated with bFGF – GH, or GH, 7 days after SCI. Weight loss was severe at 7 days after SCI: weight loss ratios for the bFGF – GH and the GH groups were 0.958 ± 0.020 and 0.938 ± 0.013, respectively. At the end of 9 weeks, the weights of the animals had increased to 1.322 ± 0.039 and 1.319 ± 0.034, respectively, for two groups. No statistically significant increase in the body weight ratio was observed during the entire experiment.

BBB locomotor scores 7 days after SCI were 1.0 ± 0.49 and 0.6 ± 0.34, respectively, for the bFGF – GH and the GH groups, and the intergroup difference was not statistically significant. BBB scores at 9 weeks were 10.5 ± 0.54 and 10.2 ± 0.58, respectively, for the two groups, and again no statistically significant difference between the groups was observed (Fig. 1). Repeated-measures ANOVA also failed to detect any statistically significant intergroup differences in BBB scores over the entire experiment period ($P = 0.27$).

Inclined plane testing showed that before SCI, rats could keep their body on an inclined plane at 61.04 ± 0.43° in a head-up position, 57.29 ± 0.44° in a transverse position, and 45.83 ± 0.25° in a head-down position. The differences were not statistically significant between groups at 4, 6, and 8 weeks after SCI (data not shown). The Rota-rod test also showed no statistically significant differences between groups at 4, 6, and 8 weeks after SCI (data not shown).

Analysis of the pre-injury data for the Hargreaves device revealed a mean thermal latency of 16.9 ± 0.4 seconds ($n = 18$). Thermal latency decreased to mean values of 13.5 ± 0.9 seconds at 5 weeks, 14.7 ± 1.0 seconds at 7 weeks, and 14.0 ± 1.1 seconds at 9 weeks in the bFGF – GH group, and 13.2 ± 1.0 seconds at 5 weeks, 13.9 ± 0.9 seconds at 7 weeks, and 13.4 ± 0.7 seconds at 9 weeks in the GH group. Although thermal latency decreased in both groups after SCI compared with normal pre-injury rats, the differences did not reach statistical significance. In addition, none of the differences in mean thermal latency between the groups at any time period were statistically significant.

Mechanical thresholds using a dynamic plantar aesthesiometer had a mean pre-injury value of 31.5 ± 1.4 g (Fig. 2: $n = 18$). The mean values decreased to 26.2 ± 1.5 g at 5 weeks, 27.2 ± 1.2 g at 7 weeks, and 28.5 ± 1.9 g at 9 weeks in the bFGF – GH group, and 22.9 ± 2.1 g at 5 weeks, 25.2 ± 2.0 g at 7 weeks, and 28.5 ± 2.2 g at 9 weeks in the GH group. The GH group exhibited significantly more mechanical allodynia compared with pre-injury rats at 5 and 7 weeks ($P = 0.006$ and $P = 0.021$, respectively). The decreases in mechanical thresholds in the bFGF – GH group were not statistically significant over the course of the entire experiment.

To elucidate the efficacy of bFGF – GH or GH for tissue protection or tissue sparing after SCI, we measured the area of the cystic cavity with cresyl violet staining 9 weeks after injury (Fig. 3). The differences between the groups did not reach statistical significance (Fig. 3C, $P = 0.94$).

The BDA signals rostral to the lesion epicenter were 49.1 ± 13.7 and 38.9 ± 11.9 for the bFGF – GH and GH groups, respectively (Fig. 4). The differences

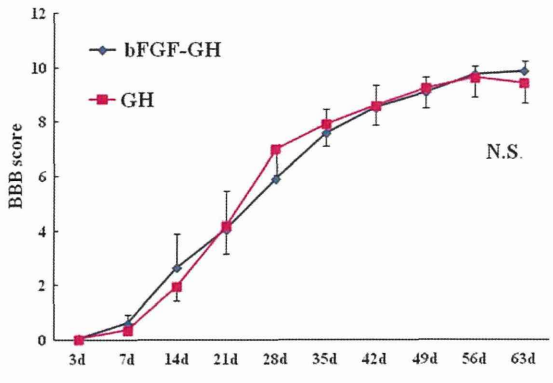


**Figure 1 BBB locomotor scores during the first 9 weeks after SCI. The differences between the groups were not statistically significant ($P = 0.27$).**

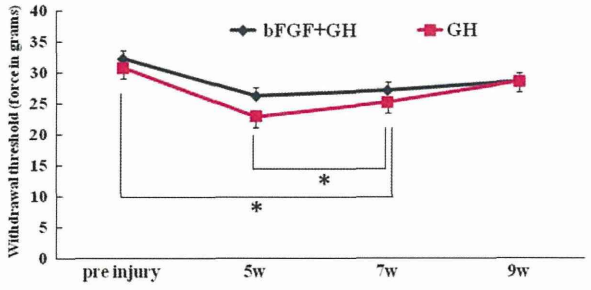


**Figure 2 Mechanical thresholds using a dynamic plantar aesthesiometer were performed pre-injury and also 5, 7, and 9 weeks after contusion. The GH group showed significantly more mechanical allodynia compared with pre-injury rats at 5 and 7 weeks ($P = 0.006$ and $P = 0.021$, respectively). However, the bFGF – GH group showed no statistically significant decrease over the entire experiment.**

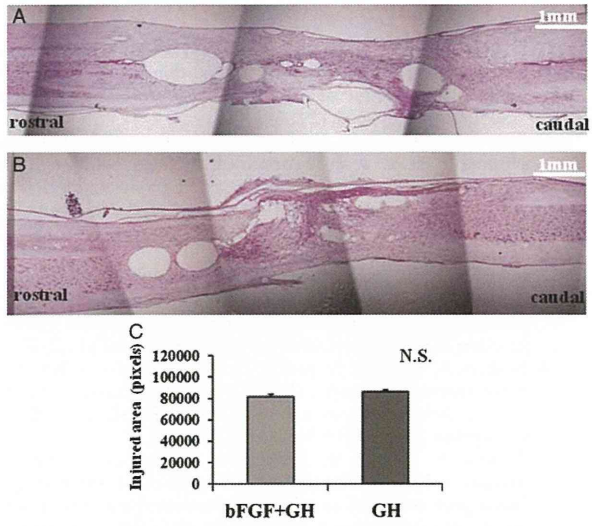


**Figure 3 Cresyl violet staining 9 weeks after SCI did not show statistically significant cavity size differences between the two groups. The cavity size of each section was analyzed. Representative figures of each group from the bFGF + GH group (A) and the GH group (B) are presented. The differences among groups did not reach statistical significance (C, $P = 0.94$). Bar = 1 mm for figures A, B.**

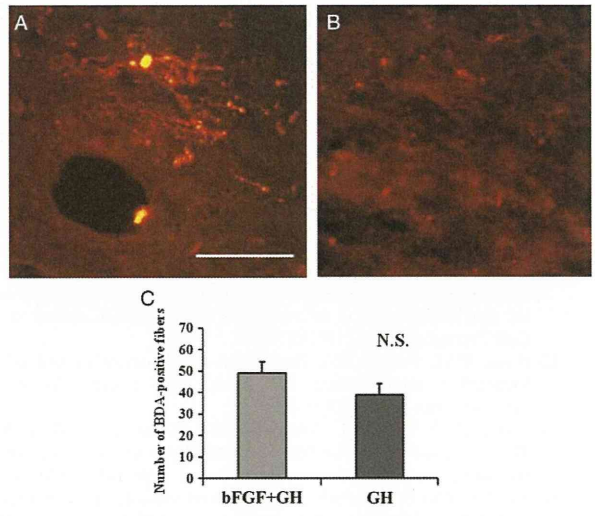


**Figure 4 Biotinylated dextran amine tracing 8 weeks after SCI. The BDA signals at the rostral edge of the lesion epicenter were analyzed. The differences between the groups did not reach statistical significance (C, $P = 0.22$). Bar = 100 μm for figures A, B.**

between the two groups did not reach statistical significance (Fig. 4C, $P = 0.22$). In the same way, we analyzed von Willebrand factor-positive signals at the lesion epicenter. Values were $23 \pm 12.0$, and $17.6 \pm 5.2$, for the bFGF – GH and GH groups, respectively. No statistically significant difference between groups was observed ($P = 0.83$).

The CGRP signals from the posterior funiculus on the rostral and caudal sides of the lesion epicenter were analyzed and compared. CGRP-positive fiber counts were $7.1 \pm 2.6$ and $35.2 \pm 6.5$ for the bFGF–GH and GH groups, respectively, and none of the differences were statistically significant ($P = 0.17$).

## Discussion

Although we injected bFGF-incorporated GH 1 week after SCI in our experimental model, the optimal timing of bFGF injection remains an unresolved issue. Several studies, though, have provided suggestive data. For instance, one study detected significant increases in various molecular forms of FGF2 protein 4 days after SCI.[13] Another study showed significant up-regulation of bFGF 3 days after SCI, when cell proliferation is maximal.[14] A third study tracked bFGF mRNA, which initially was detected 1 hour post-injury, increased between 6 hours and 3 days, declined thereafter, and returned to baseline levels by 21 days.[15] These reports together indicate that up-regulation of bFGF is maximal 3 days after SCI and gradually decreases after that, from which we deduce that in terms of timing, it is best to wait until after bFGF up-regulation has peaked before injecting bFGF. Furthermore, another study showed that epidermal growth factor and FGF2 injection immediately after SCI had no impact on BBB scores for 8 weeks.[16] On the basis of all these studies, we decided to inject bFGF-incorporated GH 7 days after SCI.

We measured BBB scores for 9 weeks after SCI and also performed Rota-rod and inclined plane testing at several time points after SCI. The locomotor measurement data showed no statistically significant recovery in this study. bFGF – GH and GH-only injections appear to have had almost identical effects on injured spinal cords. In other words, both the bFGF – GH and the GH injections may have improved the ability of injured rats to perform weight-bearing activity. While the saline-injected SCI model rats that suffered the same contusion injury of the spinal cord did not reach weight-bearing levels in their BBB scores in our previous study,[1] rats of both groups in this study were able to perform weight-bearing activity. This result implies the possibility that GH itself has neuroprotective effects. Further investigation is needed to clarify this point. To examine associated histological changes, we assessed cortico-spinal tract tracing 2 weeks before sacrifice. Comparisons of BDA signals did not show statistically significant differences between groups. This histological finding supports the locomotor assessments in which bFGF

– GH and GH-only injections showed no statistically significant recovery in this study.

We measured two types of allodynia using a Hargreaves device and a dynamic plantar aesthesiometer. We observed no statistically significant differences between groups and in comparison with pre-injury rats, in mean thermal latency using the Hargreaves device. With respect to mechanical allodynia using the dynamic plantar aesthesiometer, while the GH injection group showed significantly more mechanical allodynia than the pre-injury data, the bFGF – GH group showed no statistically significant threshold changes compared with pre-injury. Although no statistically significant differences in the posterior funiculus CGRP-positive fiber counts between rostral and caudal sides of the lesion epicenter were observed, CGRP-positive fiber counts were lower in the bFGF – GH group. The histology data thus show some correspondence with the mechanical allodynia testing data, i.e. the bFGF – GH injection group had significantly less sensitivity to mechanical allodynia.

## Conclusion

To summarize, the findings of this study revealed that the bFGF – GH group showed no statistically significant threshold changes compared with pre-injury, whereas the GH-alone group showed significantly more mechanical allodynia than the pre-injury data for that group. We had hoped to provide evidence that bFGF – GH could create a better environment for spinal cord regeneration. In the present study, although the bFGF – GH group showed almost identical amounts of recovery in comparison with GH group, we conclude that bFGF – GH created better conditions for decreasing sensory abnormalities.

## Conclusion

Although we found few significant effects of bFGF – GH therapy, our results did provide evidence that bFGF-incorporated hydrogel treatment may possibly relieve mechanical allodynia following SCI and should be comparatively safe in future clinical use.

## Acknowledgement

This research was supported by a grant-in-aid for Japanese scientific research grant 20591736.

## References

1 Furuya T, Hashimoto M, Koda M, Okawa A, Murata A, Takahashi K, *et al.* Treatment of rat spinal cord injury with a Rho-kinase inhibitor and bone marrow stromal cell transplantation. Brain Res 2009;1295:192–202.
2 Marui A, Tabata Y, Kojima S, Yamamoto M, Tambara K, Nishina T, *et al.* A novel approach to therapeutic angiogenesis for patients with critical limb ischemia by sustained release of basic fibroblast growth factor using biodegradable gelatin hydrogel: an initial report of the phase I-IIa study. Circ J 2007;71(8): 1181–6.
3 Iwakura A, Fujita M, Kataoka K, Tambara K, Sakakibara Y, Komeda M, *et al.* Intramyocardial sustained delivery of basic fibroblast growth factor improves angiogenesis and ventricular function in a rat infarct model. Heart Vessels 2003;18(2):93–9.
4 Iwakura A, Tabata Y, Miyao M, Ozeki M, Tamura N, Ikai A, *et al.* Novel method to enhance sternal healing after harvesting bilateral internal thoracic arteries with use of basic fibroblast growth factor. Circulation 2000;102(19 Suppl. 3):III307–11.
5 Aimoto T, Uchida E, Matsushita A, Tabata Y, Takano T, Miyamoto M, *et al.* Controlled release of basic fibroblast growth factor promotes healing of the pancreaticojejunal anastomosis: a novel approach toward zero pancreatic fistula. Surgery 2007; 142(5):734–40.
6 Mattson MP, Lovell MA, Furukawa K, Markesbery WR. Neurotrophic factors attenuate glutamate-induced accumulation of peroxides, elevation of intracellular $Ca^{2+}$ concentration, and neurotoxicity and increase antioxidant enzyme activities in hippocampal neurons. J Neurochem 1995;65(4):1740–51.
7 Kirschner PB, Henshaw R, Weise J, Trubetskoy V, Finklestein S, Schulz JB, *et al.* Basic fibroblast growth factor protects against excitotoxicity and chemical hypoxia in both neonatal and adult rats. J Cereb Blood Flow Metab 1995;15(4):619–23.
8 Anderson KJ, Dam LS, Cotman CW. Basic fibroblast growth factor prevents death of lesioned cholinergic neurons in vivo. Nature 1998;332(6162):360–1.
9 Teng YD, Mocchetti I, Wrathall JR. Basic and acidic fibloblast growth factors protect spinal motor neurons in vivo after experimental spinal cord injury. Eur J Neurosci 1998;10(2):798–802.
10 Itosaka H, Kuroda S, Shichinohe H, Yasuda H, Yano S, Kamei S, *et al.* Fibrin matrix provides a suitable scaffold for bone marrow stromal cells transplanted into injured spinal cord: a novel material for CNS tissue engineering. Neuropathology 2009; 29(3):248–57.
11 Johnson PJ, Tatara A, Shiu A, Sakiyama-Elbert SE. Controlled release of neurotrophin-3 and platelet derived growth factor from fibrin scaffolds containing neural progenitor cells enhances survival and differentiation into neurons in a subacute model of SCI. Cell Transplant 2010;19(1):89–101.
12 Basso DM, Beattie MS, Bresnahan JC. A sensitive and reliable locomotor rating scale for open field testing in rats. J Neurotrauma 1995;12(1):1–21.
13 Mocchetti I, Rabin SJ, Colangelo AM, Whittemore SR, Wrathall JR. Increased basic fibroblast growth factor expression following contusive spinal cord injury. Exp Neurol 1996;141(1):154–64.
14 Zai LJ, Yoo S, Wrathall JR. Increased growth factor expression and cell proliferation after contusive spinal cord injury. Brain Res 2005;1052(2):147–55.
15 Lee YL, Shih K, Bao P, Ghirnikar RS, Eng LF. Cytokine chemokine expression in contused rat spinal cord. Neurochem Int 2000; 36(4–5):417–25.
16 Jimenez Hamann MC, Tator CH, Shoichet MS. Injectable intrathecal delivery system for localized administration of EGF and FGF-2 to the injured rat spinal cord. Exp Neurol 2005; 194(1):106–19.

*Cell Transplantation*, Vol. 22, pp. 1613–1625, 2013


0963-6897/13 $90.00 + .00
DOI: http://dx.doi.org/10.3727/096368912X658791
E-ISSN 1555-3892
www.cognizantcommunication.com

# Transplantation of Bone Marrow Stromal Cell-Derived Neural Precursor Cells Ameliorates Deficits in a Rat Model of Complete Spinal Cord Transection

Misaki Aizawa-Kohama,*† Toshiki Endo,† Masaaki Kitada,* Shohei Wakao,*
Akira Sumiyoshi,‡ Dai Matsuse,* Yasumasa Kuroda,§ Takahiro Morita,*†
Jorge J. Riera,‡ Ryuta Kawashima,‡ Teiji Tominaga,† and Mari Dezawa*§

*Department of Stem Cell Biology and Histology, Tohoku University Graduate School of Medicine, Sendai, Japan
†Department of Neurosurgery, Tohoku University Graduate School of Medicine, Sendai, Japan
‡Institute of Development, Aging and Cancer, Tohoku University, Sendai, Japan
§Department of Anatomy and Anthropology, Tohoku University Graduate School of Medicine, Sendai, Japan

After severe spinal cord injury, spontaneous functional recovery is limited. Numerous studies have demonstrated cell transplantation as a reliable therapeutic approach. However, it remains unknown whether grafted neuronal cells could replace lost neurons and reconstruct neuronal networks in the injured spinal cord. To address this issue, we transplanted bone marrow stromal cell-derived neural progenitor cells (BM-NPCs) in a rat model of complete spinal cord transection 9 days after the injury. BM-NPCs were induced from bone marrow stromal cells (BMSCs) by gene transfer of the Notch-1 intracellular domain followed by culturing in the neurosphere method. As reported previously, BM-NPCs differentiated into neuronal cells in a highly selective manner in vitro. We assessed hind limb movements of the animals weekly for 7 weeks to monitor functional recovery after local injection of BM-NPCs to the transected site. To test the sensory recovery, we performed functional magnetic resonance imaging (fMRI) using electrical stimulation of the hind limbs. In the injured spinal cord, transplanted BM-NPCs were confirmed to express neuronal markers 7 weeks following the transplantation. Grafted cells successfully extended neurites beyond the transected portion of the spinal cord. Adjacent localization of synaptophysin and PSD-95 in the transplanted cells suggested synaptic formations. These results indicated survival and successful differentiation of BM-NPCs in the severely injured spinal cord. Importantly, rats that received BM-NPCs demonstrated significant motor recovery when compared to the vehicle injection group. Volumes of the fMRI signals in somatosensory cortex were larger in the BM-NPC-grafted animals. However, neuronal activity was diverse and not confined to the original hind limb territory in the somatosensory cortex. Therefore, reconstruction of neuronal networks was not clearly confirmed. Our results indicated BM-NPCs as an effective method to deliver neuronal lineage cells in a severely injured spinal cord. However, reestablishment of neuronal networks in completed transected spinal cord was still a challenging task.

Key words: Cell transplantation; Functional magnetic resonance imaging (fMRI); Bone marrow stromal cells (BMSCs); Neural progenitor cells (NPCs); Spinal cord injury (SCI)

## INTRODUCTION

Spinal cord injury (SCI) induces local neural cell death and disruption of axonal pathways. Recovery is limited, since the central nervous system (CNS) environment deters axonal growth and regeneration through the actions of myelin inhibitors and astrocytes (14,45). Among the many experimental approaches to treat SCI, cell transplantation has the potential to repair or compensate for local spinal cord damage (5,15,27,32,44).

Bone marrow stromal cells (BMSCs) constitute a possible source of cells for autologous transplantation. They can be obtained from patient bone marrow aspirates and are readily expanded in vitro, which has made them a suitable candidate for clinical applications (9,11,34). We have established a method in which neural progenitor cells can be induced from BMSCs by introduction of the Notch-1 intracellular domain (NICD) followed by culturing using the neurosphere method (10,17). These progenitor cells, that is, bone marrow-derived neural progenitor cells (BM-NPCs), successfully formed spheres that highly expressed markers related to neural progenitors. When BM-NPCs were transplanted into a rat stroke model, they were shown to differentiate into neuronal cells, reconstruct synapses with host neurons, and lead to functional recovery of the animals (17).

Received October 7, 2011; final acceptance August 15, 2012. Online prepub date: October 31, 2012.
Address correspondence to Toshiki Endo, Department of Neurosurgery, Tohoku University Graduate School of Medicine, 1-1 Seiryo, Aoba, 980-8574, Sendai, Japan. Tel: +81-22-717-7230; Fax: +81-22-717-7233; E-mail: endo@nsg.med.tohoku.ac.jp *or* Mari Dezawa, Department of Stem Cell Biology and Histology and Department of Anatomy and Anthropology, Tohoku Univeristy Graduate School of Medicine, 2-1 Seiryo-machi, Aoba-ku, 980-8575, Sendai, Japan. Tel: +81-22-717-8025; Fax: +81-22-717-8030; E-mail: mdezawa@med.tohoku.ac.jp

In the present study, we newly applied BM-NPC transplantation to a rat model of complete spinal cord transection. The aim of this study is to confirm selective neuronal differentiation of the grafted BM-NPCs in the injured spinal cord and to achieve functional recovery. A possible means of achieving recovery from the injury would be the reconstruction of disrupted neuronal circuits between grafted cells and endogenous surrounding neurons, as suggested elsewhere (1). We employed immunohistochemistry to confirm neuronal differentiation of the grafted cells in the injured spinal cord. Synaptic formation of the BM-NPCs was evaluated with synaptophysin and postsynaptic density (PSD)-95. Retrograde tracing with fluorogold (FG) was utilized to see whether the BM-NPCs extended neurites across the transected portion of the spinal cord. We also used functional magnetic resonance imaging (fMRI) of the brain using blood oxygenation level-dependent (BOLD) contrast (12,13,30,40) to test sensory recovery and detect reestablishment of ascending neurotransmission across the injury. Behavioral analysis was included to evaluate locomotor recovery.

## MATERIALS AND METHODS

### *Preparation of Marrow Stromal Cells and Neural Induction*

All animal experiments were approved by the Animal Studies Ethics Committee of Tohoku University Graduate School of Medicine. Experimental procedures are presented in Figure 1. Numbers of animals used for each experiment were listed in Table 1. Rat BMSCs were isolated from adult female 10-week-old Wistar rats (CLEA Japan, Inc., Tokyo, Japan) according to methods described previously (4). Cells were maintained in α-minimum essential medium (α-MEM; Sigma, St. Louis, MO, USA) containing 10% fetal calf serum (FCS; Hyclone, Inc., Logan, UT, USA) and kanamycin (Wako Pure Chemical industries, Ltd., Osaka, Japan) at 37°C with 5% carbon dioxide. Next, the cells were transfected with a vector (pCI-neo-NICD) containing the mouse NICD (10). The NICD cDNA coded for a transmembrane region that included a small fragment of extracellular domain followed by a sequence encoding the entire intracellular domain of mouse Notch (initiating at amino acid 1,703 and terminating at the 3′-untranslated sequence).

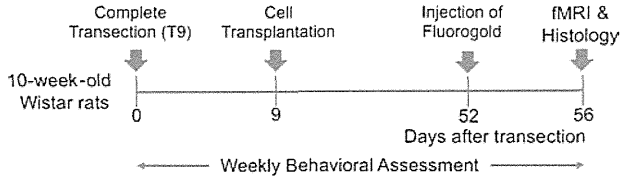


**Figure 1.** Experimental procedure. See Materials and Methods for detailed information. fMRI, functional magnetic resonance imaging.

**Table 1.** The Number of Animals per Experiments

| | BBB Locomotor Scale | Fluorogold Tracing | fMRI Study | Total |
|---|---|---|---|---|
| Vehicle group | $n=14$ | $n=4$ | $n=6$ | $n=14$ |
| BM-NPCs group | $n=10$ | $n=4$ | $n=6$ | $n=10$ |

BBB, Basso, Beattie, Bresnahan; BM-NPCs, bone marrow-derived neural progenitor cells; fMRI, functional magnetic resonance imaging.

This fragment was subcloned into a pCI-neo vector (Promega, Madison, WI, USA) and was transfected with BMSCs using Lipofectamine LTX (Invitrogen, Carlsbad, CA, USA) and selected using G418 (Invitrogen) for 5 days according to the manufacturer's instructions (10).

### *Induction of BM-NPCs*

After G418 selection, rat NICD-transfected cells were washed and cultured in α-MEM containing 10% FCS for 2 days for recovery. The efficacy of NICD transfection was 98.8±0.8%, which is consistent with the previous report (10). During the expansion and recovery of transfected cells after G418 selection, green fluorescent protein (GFP) lentivirus (provided by Dr. D. Trono, Lausanne, Switzerland) was added to the culture medium for labelling purposes (29,39). Efficacy of GFP transfection was calculated three times. After recovery, the cells were washed and cultured in neurobasal medium supplied with B27 supplement (Invitrogen), 20 ng/ml of basic fibroblast growth factor and epidermal growth factor (both R&D Systems, Minneapolis, MN, USA) (17) at a cell density of 100,000 cells/ml on low cell-binding dishes (Nalgene Nunc, Rochester, NY, USA). After 8 days, generated spheres, namely BM-NPCs, were resuspended in Neurobasal medium to a concentration of approximately 30,000 cells/μl and transplanted to the injured rat spinal cord.

### *Immunocytochemistry*

Spheres were fixed with 4% paraformaldehyde in 0.1 mol/L phosphate-buffered saline (PBS; both from Wako Pure Chemical Industries), collected by centrifugation, embedded in optimal cutting temperature (OCT) compound (Sakura Finetek Japan, Tokyo, Japan), and cut into 10-μm-thick sections using a cryostat (CM1850; Leica, Wetzlar, Germany). Samples were incubated with blocking solution containing 5% normal goat serum (Vector Laboratories, Burlingame, CA, USA), 0.1% Triton X-100 (Sigma), and 0.3% bovine serum albumin (BSA; Sigma) in 0.1 mol/L PBS at room temperature for 30 min. Samples were then incubated with primary antibodies in blocking solution overnight at 4°C. After three washes with 0.1 mol/L PBS, samples were incubated with secondary antibodies for 2 h at room temperature, followed by counterstaining with 4′,6-diamidino-2-phenylindole (DAPI) (for nuclear staining,

1:500; Sigma). The following primary antibodies were used for immunocytochemistry: anti-sex-determining region Y box 2 (Sox2; rabbit IgG, dilution 1:5,000; Chemicon, Temecula, CA, USA), anti-neurogenic differentiation (NeuroD; rabbit IgG, 1:200; Chemicon), anti-nestin (mouse IgG, 1:400; BD Pharmingen, San Jose, CA, USA), and anti-musashi (rabbit IgG, 1:200; Millipore, Billerica, MA, USA), anti-neuron-specific nuclear antigen (NeuN) (mouse IgG, 1:200; Chemicon), anti-glial fibrillary acidic protein (GFAP) (mouse IgG, 1:300; Sigma-Aldrich), and anti-oligodendrocyte marker 4 (O4; mouse IgM, 1:20; Millipore). These primary antibodies were detected with Alexa 488-conjugated anti-rabbit IgG or anti-mouse IgG antibodies (Molecular Probes, Invitrogen, Eugene, OR, USA) or Alexa 546-conjugated anti-rabbit IgG (1:500; Molecular Probes) or biotin-conjugated anti-mouse IgM (1:500; Jackson ImmunoResearch, West Grove, PA, USA) and streptavidin Alexa Fluor 488 (1:500; Molecular Probes) and streptavidin Alexa Fluor 680 (1:200; Molecular Probes). Percentages of immunopositive cells were calculated by comparing the cell numbers with the number of DAPI-positive cells. Cells in five fields, each including 100–500 cells, were counted in three independent cultures. Results were averaged and expressed as mean±SEM.

*Complete Transection of the Midthoracic Spinal Cord (T9)*

Adult, 10-week-old female Wistar rats weighing 200±20 g underwent complete transection of the spinal cord at the midthoracic level. Under isoflurane anesthesia (Wako Pure Chemical Industries), a laminectomy was performed at the T8–9 level. The spinal cord was exposed and transected completely using microscissors. Possible remaining adhesions were cut with a scalpel, and the rostral and caudal stumps were carefully lifted to verify complete transection. The dural incision was left open. Muscle and skin were sutured separately. The urinary bladder was emptied manually twice daily during the first week and once daily thereafter for 8 weeks.

*Transplantation of BM-NPCs*

Nine days after SCI rats were randomly assigned to groups receiving vehicle (vehicle group; $n=14$) or induced neural progenitor cells (BM-NPC group; $n=10$). Based on a previous report, the timing of transplantation was chosen to avoid delivering cells in an acute inflammatory stage following the injury or in chronic stage in which glial scar tissues would hinder regeneration of axons (31). The numbers of animals used in each experiment are shown in Table 1. Rats were reanesthetized and the thoracic spinal cord was carefully reexposed. Four injections were made with a depth of 1 mm, at 2 mm rostral and caudal of the lesion, and 0.5 mm left and right from the midline. At each site, 2.5 μl of cell suspension or vehicle (α-MEM; Sigma) was infused stereotactically using a Hamilton microsyringe attached to a glass micropipette at the rate of 0.5 μl/min (Hamilton, Reno, NV, USA). A total of 300,000 BM-NPCs were delivered to the spinal cord. The needles were left in the place for 1 min following each injection to prevent cells leaking from the site (2).

*Immunohistochemical Analysis*

Eight weeks after SCI, animals were anesthetized with an overdose of pentobarbiturate (Wako Pure Chemical Industries) and perfused transcardially with 4% paraformaldehyde in 0.1 mol/L PBS. Spinal cords were removed and embedded in OCT compound, and axial or sagittal slices were cut. Each spinal cord slice was cut into 10-μm sections using a cryostat. In three animals in each group, sagittal sections were used for neurofilament staining. The other immunohistochemical analyses were performed with axial slices. For immunostaining, the sections were washed with PBS and incubated with 5% normal goat serum, 0.3% Triton X-100, and 0.3% BSA in PBS (blocking solution) at room temperature for 30 min to block nonspecific binding. The slides were incubated with primary antibodies diluted in the blocking solution and incubated overnight at 4°C. After three washes with PBS containing 0.05% Triton X-100, the slides were incubated with secondary antibodies for 2 h at room temperature, followed by counterstaining with DAPI, which was diluted in PBS containing 0.1% Triton X-100. Sections were immunolabeled with the following primary antibodies: anti-neuron-specific class III β-tubulin (antibody name: Tuj-1; mouse IgG, 1:200; Sigma-Aldrich), anti-NeuN (mouse IgG, 1:200; Chemicon), anti-GFAP (mouse IgG, 1:300; Sigma-Aldrich), anti-O4 (mouse IgM, 1:20; Millipore), anti-synaptophysin (mouse IgG 1:1000; Chemicon), anti-PSD-95 (mouse IgG2a 1:100; Chemicon), anti-neurofilament (rabbit IgG, 1:200; Chemicon), and anti-GFP (chicken IgG, 1:1,000; Abcam, Philadelphia, PA, USA). Secondary antibodies were anti-mouse Alexa Fluor 568 (1:500; Molecular Probes), biotin-conjugated anti-chicken IgG (1:200; Jackson ImmunoResearch), anti-rabbit Alexa Fluor 568 (1:500; Molecular Probes), and streptavidin Alexa Fluor 488 (1:500; Molecular Probes). After immunolabeling, the samples were inspected under a confocal microscope system (C1si; Nikon, Tokyo, Japan). Using three animals in the BM-NPC group, transplanted cells in 20 fields in each cryosection were counted to confirm the survival of GFP-positive transplanted cells and evaluated the differentiation of BM-NPCs in the injured spinal cord. Results were averaged and expressed as mean±SEM.

*Tracing Study*

To label regenerated axons, FG (Fluorochrome, Denver, CO, USA) was injected into the spinal cord 4 days before the rats were killed (41). Using four rats in each group,

4% FG was injected into the spinal cord 10 mm caudal to the transected site over a period of 3 min using a microsyringe (24). After transcardiac perfusion, sections in the axial plane in the thoracic spinal cord including rostral and caudal ends of the transected site, cervical spinal cord, and the brain were stained with anti-FG (rabbit IgG, 1:200; Millipore) as a primary antibody and Alexa 568-conjugated anti-rabbit IgG (1:500, Molecular Probes) as a secondary antibody. Numbers of FG-positive grafted cells were counted at the rostral boundary of the transected spinal cord up to 5 mm from the transected stump. Results were averaged and expressed as mean ± SEM.

*Locomotor Scale*

Motor function in the hind limbs of all animals ($n=24$) was assessed using the Basso, Beattie, Bresnahan (BBB) locomotor rating scale on the day after injury and each week for 8 weeks after injury (6). Hind limb function was scored from 0 (flaccid paralysis) to 21 (normal gait) as a blind basis. The BM-NPC and vehicle groups were compared using multiple measurement analysis of variance (ANOVA) followed by Tukey's test. All values are given as mean ± SEM. For comparison, we also applied Mann–Whitney $U$ test to evaluate BBB locomotor scale. A value of $p<0.05$ was considered statistically significant.

*Functional MRI*

*Animal Preparation.* Rats subjected to spinal cord transection and BM-NPC transplantation ($n=6$) or vehicle injection ($n=6$) underwent brain fMRI 8 weeks after injury, as described (25,40,42). Rats were first anesthetized with isoflurane (2.5% during induction and intubation) mixed with oxygen (30%) and air (70%). Rats were intubated and mechanically ventilated using a rodent ventilator (SAR-830AP Ventilator; CWE, Ardmore, PA, USA). A pair of small needle electrodes (NE-224S; Nihon-Koden, Tokyo Japan) was implanted subcutaneously in the left hind limb of each animal to deliver electrical stimulation. To confirm correct placement of the electrodes, a short sequence of current pulses (0.5 mA) was applied outside the magnet to evoke light muscle twitches. Next, a bolus of α-chloralose (20 mg/kg) (Sigma-Aldrich) was injected through the tail vein catheter, and 10 min later, the isoflurane was discontinued. Anesthesia was continued with α-chloralose infusion (20 mg/kg/h), and pancuronium bromide (2 mg/kg/h; Sigma-Aldrich Japan, Inc., Tokyo, Japan) was added for muscle relaxation. Rectal temperature was monitored and maintained at 37 ± 0.5°C using a water-circulating pad (CLEA Japan, Inc.) during the experiment.

*fMRI Recordings.* All MRI data were acquired using a 7T Bruker PharmaScan system (Bruker Biospin, Karlsruhe, Germany) with a 38-mm diameter birdcage coil. Prior to all MRI experiments, we first performed global magnetic field shimming inside the core and later completed shimming at the region of interest (ROI) by using a point-resolved spectroscopic protocol (37). Line width (full width at half maximum) at the end of the shimming procedure ranged from 15 to 20 Hz in the ROI (~300 μl). For the rat experiment, BOLD signals were obtained using gradient echo planar imaging (EPI) with the following parameters: repetition time (TR) = 1500 ms, echo time (TE) = 15 ms, spectral band width (SBW) = 250 kHz, field of view (FOV) = 25 × 14 mm$^2$, matrix size = 125 × 70, number of slices = 7, slice thickness = 1 mm, slice gap = 0 mm, number of volumes = 427, and number of dummy scans = 4.

*Electrical Stimulation.* A block design paradigm consisting of 10 blocks was employed, in which each block comprised 13 image packages of stimulation followed by 27 image packages of the resting condition. Electrical pulses were produced using a generator (SEN-3401; Nihon Koden) and an isolator (SS-203J, Nihon Koden). Pulsed currents of 10.0 mA with 0.3 ms duration and a constant frequency of 3 Hz were first delivered to the left hind limb of animals.

*fMRI Data Analysis.* Using statistical parametric mapping software (SPM2, Wellcome Department of Cognitive Neurology, London, UK), we normalized an individual rat's brain to the rat brain atlas template using the T2-weighted images (38). Spatial smoothing was performed using a Gaussian kernel of 0.6 mm full width at half maximum. Single-subject analysis was performed with a critical $T$ value for each voxel calculated for the significance level of $p<0.001$. In response to the hind limb stimulation, volumes of significant clusters in cortex were compared between the groups using the Student's $t$ test, after normal distribution of the data sets were confirmed using Kolmogorov–Smirnov test. We counted fMRI signals in bilateral somatosensory cortex. Activations were counted separately in the hind limb territory of the primary somatosensory cortex as well as the cortical areas medial and lateral to the hind limb area as defined in the rat atlas (36). Time course of BOLD signals (%) was depicted for the BM-NPC transplantation groups using a voxel [2.6, −2.0, −1.0] located in the original hind limb territory of primary somatosensory cortex (36). A single time course was created by averaging across all stimulation periods as described elsewhere (35). All values are given as mean ± SEM.

## RESULTS

*Grafted BM-NPCs Survived and Differentiated Into Neuronal Lineage Cells in the Injured Spinal Cord*

In neurosphere culture, the NICD transfected BMSCs formed spheres. We examined the expression of nestin, NeuroD, Sox2, and musashi to determine whether these

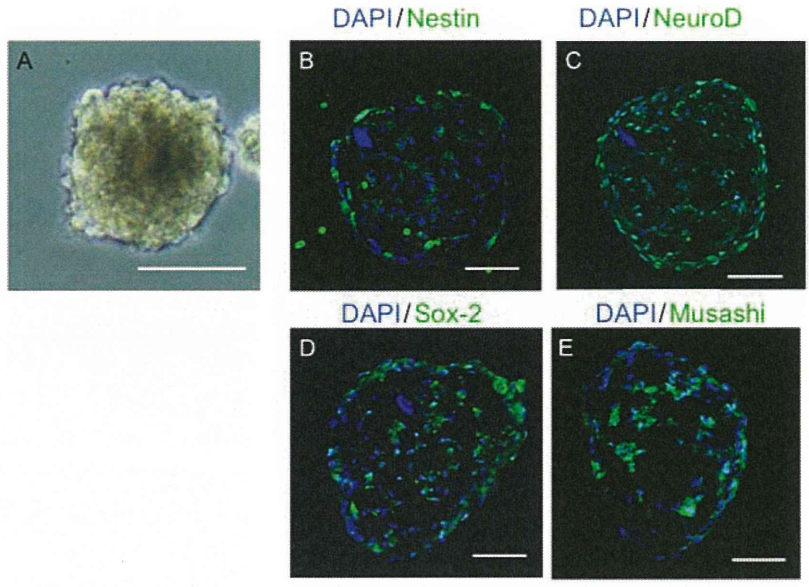


**Figure 2.** Induction of bone marrow-derived neural progenitor cells (BM-NPCs). (A) A phase contrast microscopy demonstrating BM-NPCs forming spheres on a low cell-binding dish. (B–E) Immunofluorescence images. Expression of nestin (B), neurogenic differentiation (NeuroD) (C), sex-determining region Y box 2 (Sox2) (D), and musashi (E) was confirmed. DAPI, 4′,6-diamidino-2-phenylindole. Scale bars: 50 μm.

spheres contained cells with neural progenitor cell markers. Spheres contained high percentages of cells positive for nestin (62.5±2.1%), NeuroD (82.3±2.1%), Sox2 (87.8±1.4%), and musashi (81.9±1.4%) (Fig. 2), while none of the cells were positive for NeuN (not shown). In addition, spheres did not contain cells positive for GFAP and O4 (not shown) suggesting that, consistent with the previous report, cells committed to the glial fate were not present in the sphere (17,28).

Next, BM-NPCs were transplanted into the injured spinal cord. Over 7 weeks after transplantation, no tumor formation was observed in any of the 10 spinal cords by inspection or histological analysis. Continuity of the spinal cord parenchyma was confirmed macroscopically and by neurofilament immunohistochemistry (Fig. 3A, B). Grafted cells were recognized in vivo by positive labeling of GFP. After transplantation of BM-NPCs 2 mm rostral and caudal to the transected portion of the spinal cord, grafted cells were confirmed to be located as far as 6 mm from the center of the injury (Fig. 3C–F). The total numbers of GFP-labeled cells were $8.02\pm0.71\times10^3$ in the injured spinal cord. Efficacy of GFP transfection was 45.0±4.4% in vitro. Accurate assessment of donor cell survival can only be pursued by counting all of the GFP signals in every spinal cord section. In this sense, there is a limitation of assessing the true measure of donor cell survival in our count, but the ratio of transplanted cells that survived in the injured spinal cord was estimated to be roughly 5.9%.

Importantly, BM-NPCs survived and showed low capacity for differentiating into astrocytes in the injured spinal cord. The frequencies of βIII tubulin (antibody Tuj-1)- and NeuN-positive cells among GFP-positive cells were 77.2±2.6% (Fig. 4A–E) and 36.0±3.2% (Fig. 4F–I), respectively. Nestin-positive cells were observed among the GFP-positive cells at the ratio of 9.7±2.0% (Fig. 4J–M), while the ratio of GFAP-positive cells was 2.9±0.9% (Fig. 4N–Q). O4 positive cells could not be detected (not shown). These observations suggested that the majority of the transplanted BM-NPCs became neuronal marker-positive cells. Moreover, the frequency of nestin-positive cells, which was 62.5±2.1% in vitro and 9.7±2.0% in vivo, indicated advancement of differentiation of the transplanted cells within the injured spinal cord, as nestin is potential indicator of neural differentiation (43). Spheres contained no cells positive for NeuN, while the frequency of NeuN-positive cells among GFP-positive cells increased in vivo, which also supported differentiation of the grafted cells. Transplanted cells were also found to express the synaptic marker synaptophysin (Fig. 5). Among GFP-positive cells, 24.2±2.2% were positive for synaptophysin. It was noted that synaptophysin was localized predominantly next to GFP-positive transplanted cells in a punctate pattern (Fig. 5). To further assess the synaptic formation between the transplanted cells and the host cells, immunohistochemistry for PSD-95 was performed (8,22). PSD-95 labeling was adjacent to the synaptophysin-positive signal in the transplanted cells (Fig. 6).